J6.4 NO_X PRODUCTION BY LABORATORY SIMULATED TLES

Harold Peterson[1], Matthew Bailey[2], John Hallett[2], William Beasley[3]
1- NASA-Marshall Space Flight Center, Huntsville, AL, USA
2- Desert Research Institute, Reno, NV, USA
3- University of Oklahoma, Norman, OK, USA

1. Introduction

Though it has been known for a long time that lightning produces oxides of nitrogen (NO_x), serious research on the subject has been undertaken only in the last 30 years or so. The study of NO_x first achieved prominence when it was found that NO is an important precursor to photochemical smog (Cohen 2003). Also, N_2O can be split by sunlight, releasing oxygen atoms (O) that lead to tropospheric ozone (O_3) production (Vollhardt 1999). This process by itself does not lead to a net production of O_3, but leads to increased O_3 concentrations when hydrocarbons such as those released in the exhaust of vehicles are present (Oke 1999). Out of these oxides of nitrogen, NO and NO_2 have been linked to the destruction of stratospheric ozone (Cohen 2003). A chemical inventory of global NO_x would be needed to determine whether lightning-produced NO_x has any effects on ozone in either atmospheric layer.

Corresponding author address: Harold Peterson, National Space Science and Technology Center, 320 Sparkman Drive, Huntsville, AL 35805; email: peter188@unr.nevada.edu

1.1 *Formation of NO_x by TLEs*

There are high concentrations of NO_x present in the middle atmosphere (Callis 2002). For example, Gordley et al (1996) found NO_2 mixing ratios of 1 ppb at 30 mb, increasing to 8 ppb at 10 mb. NO_2 vertical column densities in the stratosphere are greatest in the polar daytime. In contrast, they are lowest in the polar winter and in the tropics (Wenig 2004). The source of this NO_x is currently unknown. Experimental evidence is provided in support of the hypothesis that blue jets, red sprites, and other transient luminous events (TLEs) can be a source of middle atmosphere NO_x. From these results, an estimate of global NO_x production by TLEs is calculated. A similar study by Rozanov et al (2005) found that NO_y produced by energetic electron precipitation reduced ozone levels by 5% at mid-latitudes, increasing to a 30% reduction near the South Pole. This had the additional effect of reducing stratospheric and tropospheric temperatures. This suggests that if TLEs do prove to be a significant source of middle atmosphere NO_x, they need to be taken into account in future NO_x budget estimates.

2. Experimental Apparatus

2.1 *Chamber and electrical circuit*

For these experiments discharges were conducted in an evacuated chamber consisting of two metal plates separated by a hollow acrylic cylinder (Figures 1, 2). In the laboratory setting, chamber pressure is easily controlled to within 1 mb for pressures between 10 mb and room pressure, and to within 0.1 mb for lower pressures. In the low-energy configuration, the bottom electrode (cathode) was brass, while the top electrode (anode) was a copper wire, with a 5 cm gap between electrodes. In the high-energy configuration, both electrodes were brass, with a 3 cm gap between electrodes.

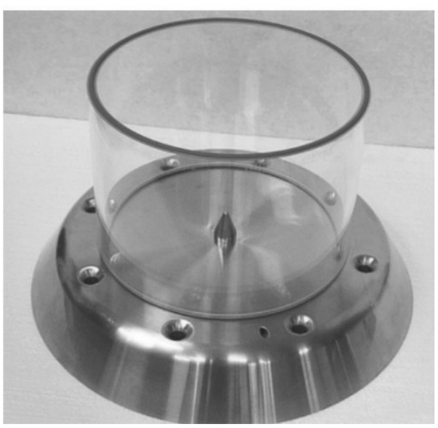

Figure 1: Pressure-controlled discharge chamber, with bottom plate attached

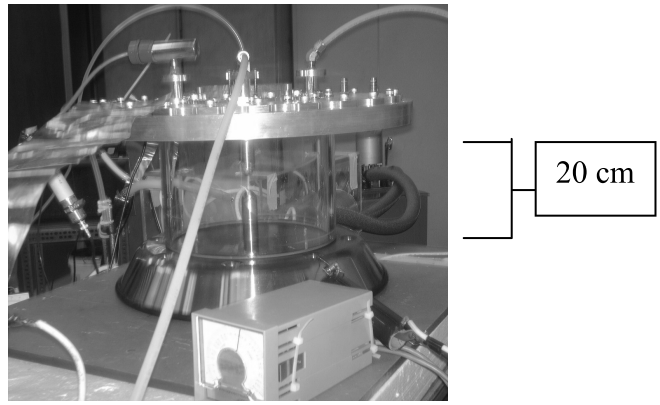

Figure 2: Chamber with both plates attached

A DC power source was used to establish an electric field with voltages between 0 and 30 kV. The electric field can be built up over any user-specified period of time, or a relay switch connected to a capacitor can send the voltage to the bottom plate of the chamber abruptly. The current from the power source is sent one of two ways. First, it can be sent through a series of copper sulfate solution resistors directly to the bottom plate of the chamber, which can be set as either positive or negative depending on the polarity of the power supply. Alternately, the current can be sent through a series of ceramic resistors to a ceramic capacitor, where the charge is stored until the switch connecting the capacitor to the bottom plate is closed (Figure 3). Current values during the discharges were measured using a current-viewing resistor, or CVR. The top plate of the chamber is grounded.

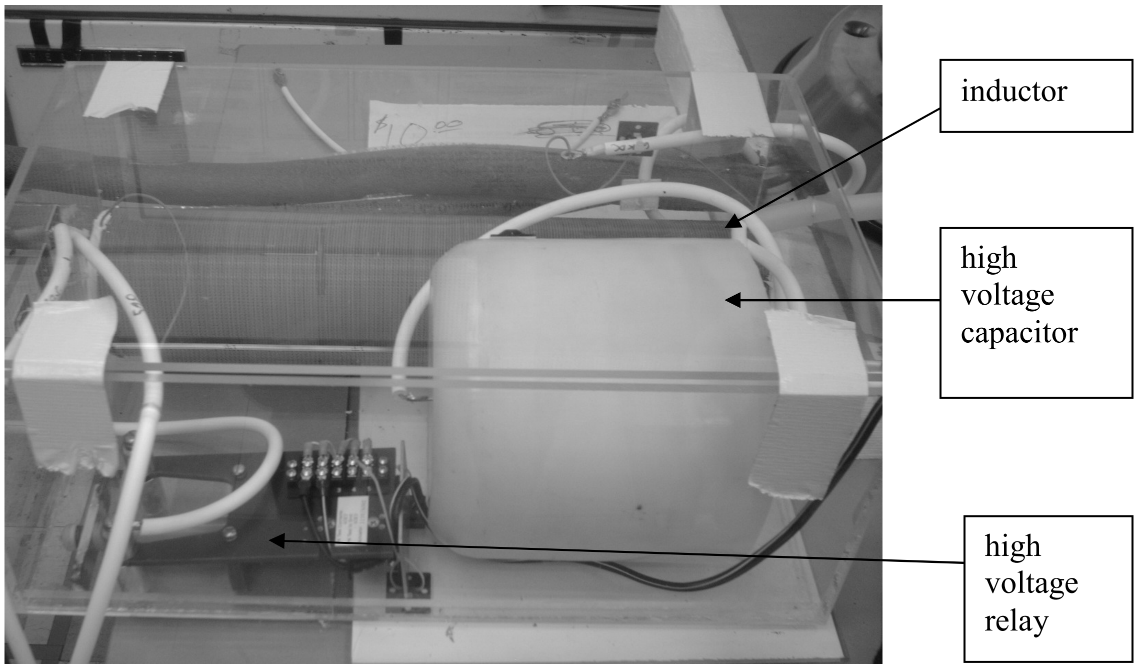

Figure 3: Capacitor, inductor and switching device

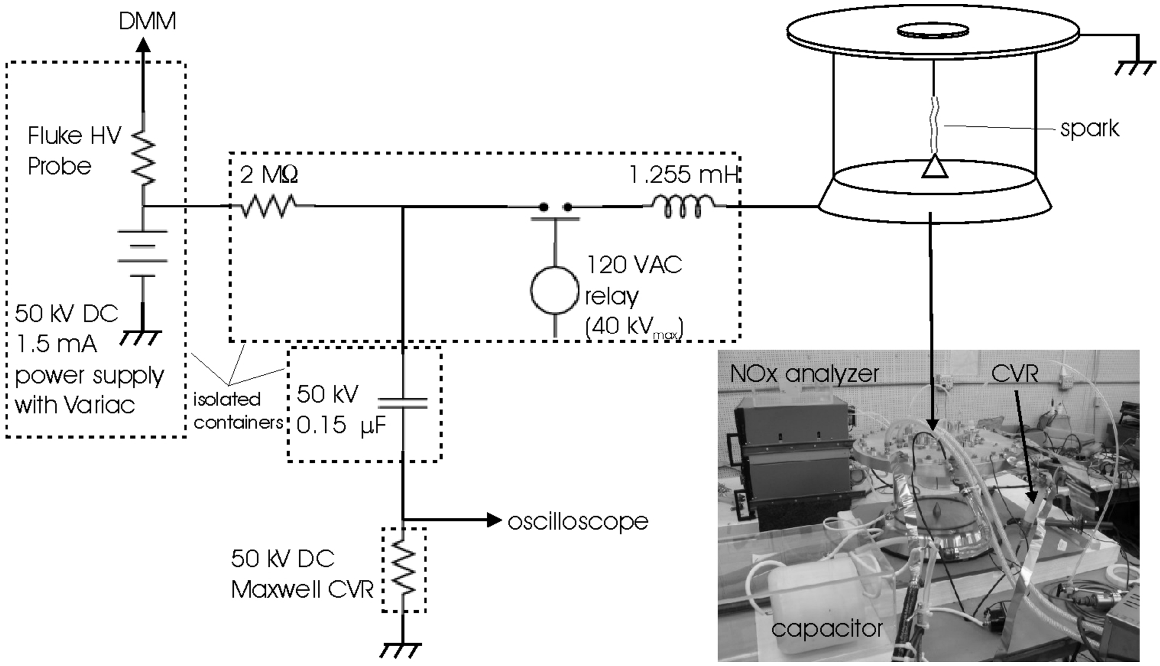

Figure 4: Chamber with electrical components shown. The NOx analyzer, capacitor and current viewing resistor (CVR) are indicated.

During the discharge, a fraction of the energy stored in the capacitor prior to discharge, given by ½CV^2, is dissipated through resistive losses in the circuit rather than in the spark gap, the fraction lost increasing with increasing voltage and current. Wang et al (1998) found that over 95% of electrical energy delivered by their Marx bank was dissipated in the external circuit and resistors rather than in the spark gap used in their experiment. Therefore, NO_x production efficiency is given by the energy in the spark gap, calculated by integrating the product of voltage and current over the time of discharge. Current waveforms measured with a current viewing resistor and with an oscilloscope are shown in Figure 5. The discharge is said to end when measured current has returned to background levels. This allows one to ignore time dependent integrated inductive effects, which are zero at the beginning and end of the discharge, leaving only resistive losses as calculated through standard RCL time dependent circuit analysis.

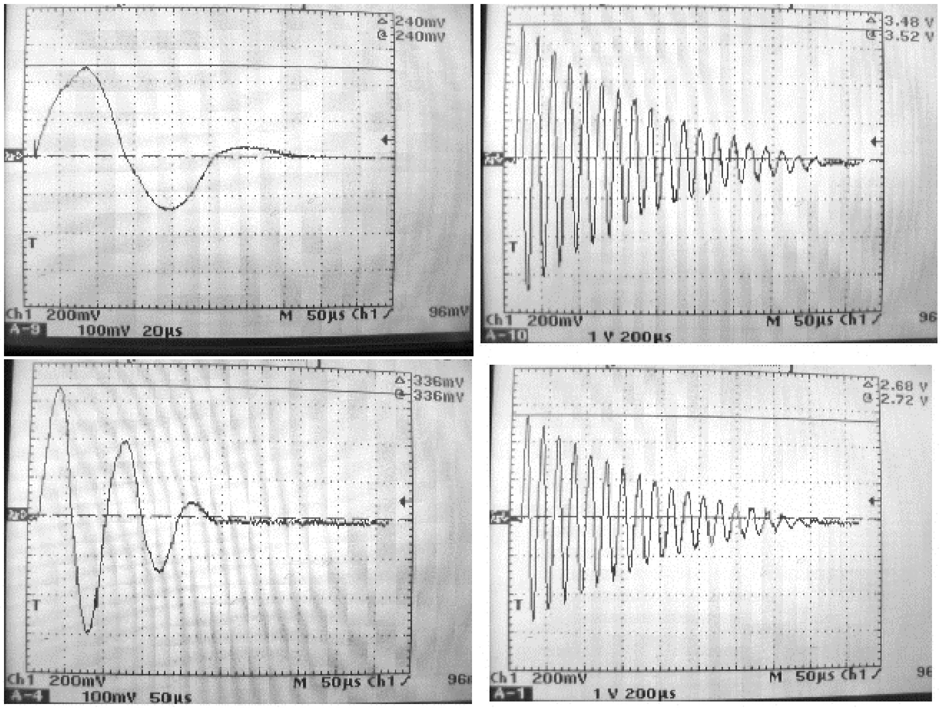

Figure 5: Sample waveforms of electrical current, as measured during laboratory discharges. High precision attenuators were used to keep CVR signals within the input parameters of the oscilloscope over the range of discharge currents (up to 350 A). Measured currents were scaled up to true values using attenuator values. The oscillations in current are modeled using an RLC circuit. Integrating the product of this current with the discharge voltage gives the energy present in the electrical discharge.

For the circuit used in this study, it was determined that the ratio of energy stored in the capacitor to the energy dissipated in the discharge was as much as 7 for the largest currents at 500 mb, but was only 1.1 for the smallest currents at 1 mb. These results are obtained by comparing the energy stored for some voltage, $\frac{1}{2}CV^2$, with the energy dissipated in the resistive and inductive elements of the circuit as given in Equation 1.

$$E(\text{joule}) = \int I(t)^2 R\, dt - L/2 \int (I\, dI/dt)\, dt' \qquad (1)$$

The inductive term is conveniently zero at both t = 0 and t = ∞ (or after the oscillation has thoroughly damped out), so this term drops out of the calculation. Defining a dimensionless damping constant,

$$\rho = \tfrac{1}{2} R\sqrt{C/L} \qquad (2)$$

the current is given by

$$I = (V/R)2\rho(1-\rho^2)^{-\frac{1}{2}} \exp(-\rho\omega_o t) \sin[(\omega_o(1-\rho^2)^{\frac{1}{2}} t] \qquad (3)$$

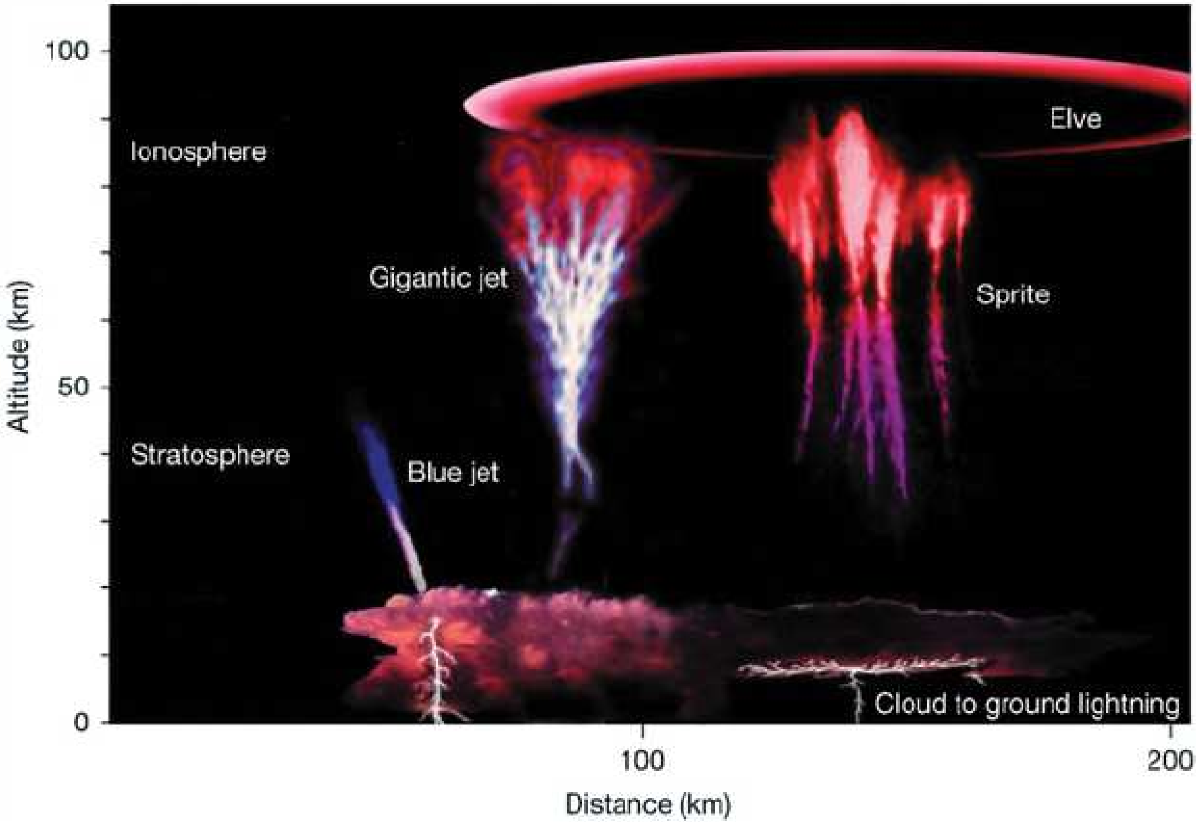

where ω_o is the undamped frequency of the circuit, $\omega_o = 1/\sqrt{(L/C)}$. Squaring the current and integrating over the apparent decay times shown in the wave forms yields the energy dissipated in the external circuit, which when subtracted from the stored energy yields the energy discharged in the gap.

II. Discharge Characteristics

Using the 30 kV power supply and the system described, the following discharges shown were used as approximate models of natural TLEs (Figure 6) and glow discharges in the chamber. Images were captured with a simple digital camera in movie mode at a rate of about 30 frames per second. While slow in speed the camera was able at times to capture pre- and post-discharge phenomena.

Figure 6: Summary of TLEs in the atmosphere from Pasko (2007). Laboratory discharges were used to simulate blue jets and red sprites.

Discharges at pressures greater than 100 mb (500 mb maximum pressure) were bright white in color like typical tropospheric CG and IC discharges, though some contained a hint of blue. A transition region produces sparks that have a white core surrounded by a mix of both blue and red emissions which increase with decreasing pressure as seen on the right hand side of Figure 7. In sprites the red light is emitted by excited nitrogen molecules (Inan 2002). Specifically, the N2 1 PG (3-1) transition emits photons of wavelength 762.7 nm (Yair 2004). In blue starters, a type of TLE related to blue jets, the blue color is from the 427.8 nm first negative transition in N_2^+ molecules (Pasko 2002 B). Below 5 mb and at relatively low current, the discharges fan out from the anode toward the cathode, where it encounters a dark zone known as a cathode dark region just before attaching to the cathode. These discharges are bluish in color around 3 mb, and tend toward a mix of blue and red down to 0.5 mb (upper left, Figure 7). Observations show a transition occurs in sprites from a lower streamer region, to a transition region with a mean altitude of 78.2 km and one to two km in depth (Gerken 2005), to an upper diffuse region (Pasko 2002 A). While the chamber pressure in these discharges is higher than in the transition region of sprites, the current densities are similar. Pasko (2007) reported that individual streamers last for 1-2 ms within a sprite, as compared to 0.53 ms for model results. This is consistent with measurement of blue emissions in red sprites, which last less than 1 ms, and is also consistent with the ringdown times of discharge waveforms shown in Figure 5, between 1.0 and 1.1 ms. These blue emissions are concurrent with energies sufficiently high to ionize and dissociate nitrogen molecules.

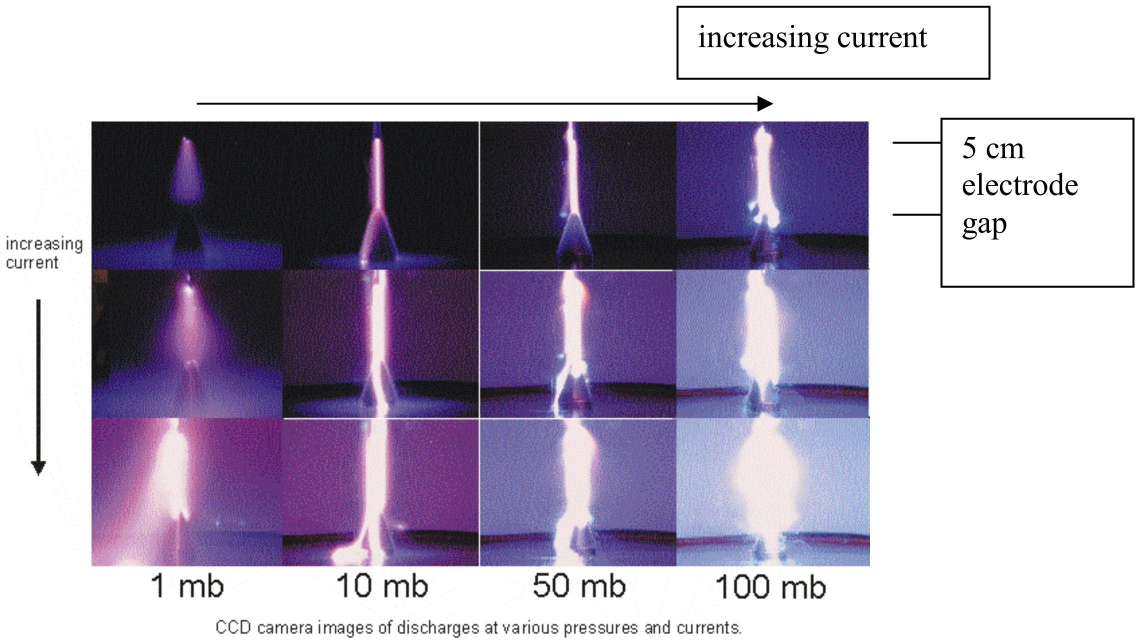

Figure 7: CCD camera images of discharges over a wide variety of pressures. Discharges occurring at lower pressures were lower in energy due to a lower voltage needed for electric field breakdown, leading to a decrease in relative luminosity. For the same pressure, an increase in current (corresponding to a higher voltage across the plates) caused the discharge to bypass the bottom electrode and originate from the bottom plate.

conditions found in the vertical middle of the blue jet.

Figure 8 shows an example of a blue jet above a thunderstorm. The cloud top is approximately 200 mb, while the top of the blue jet is about 1 mb. The 10 mb discharge simulates the pressure and electric field

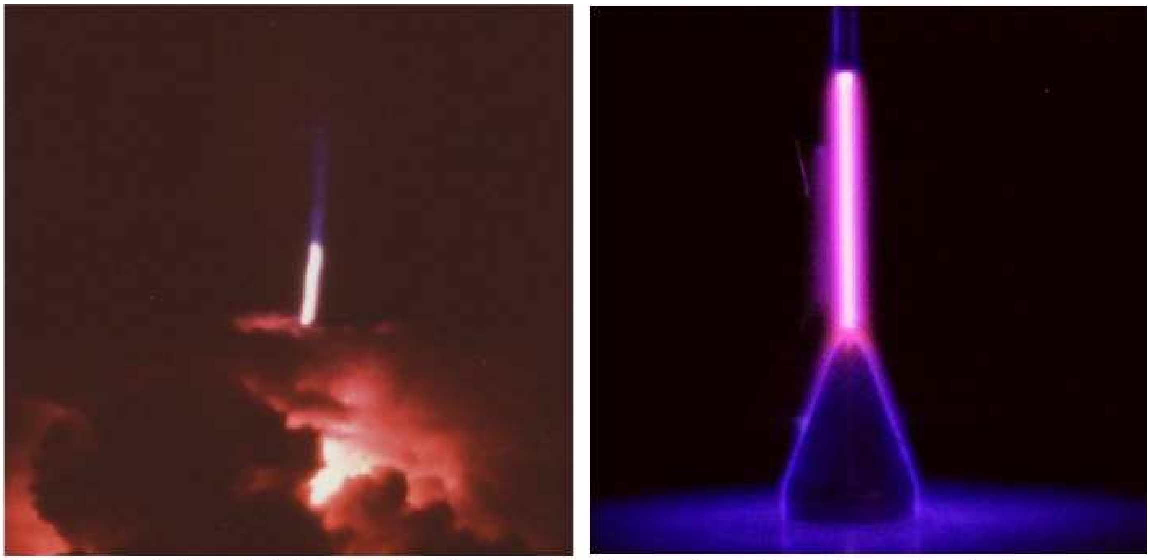

Upwards blue jet from the top of a thunder cloud and a laboratory discharge under similar pressure and current conditions.

Figure 8: Comparison between a chamber discharge and a blue jet. The chamber pressure is 10 mb. For comparison, the pressure at the top of a blue jet is on the order of 1 mb, and the base pressure is on the order of 100 mb. The scale of the chamber is the same as in Figure 6. The length of a typical blue jet is 30-40 km.

2.2 *NO_x measurement*

Nitric oxide and nitrogen dioxide concentrations (hereafter collectively referred to as NO_x) were measured using a Thermo Environmental Instruments Model 42 Chemiluminescence NO- NO_2 - NO_x Analyzer (hereafter referred to as the NO_x analyzer). NO_x molecules were made to be chemiluminescent by combining a gas sample with ozone, resulting in a fraction of NO_x molecules in excited states. Resultant photon emissions were measured using photomultiplier tubes (PMTs), and photon count was converted internally to NO_x concentration. Measurements are time-multiplexed for NO and NO_x concentration, with NO_2 concentration equaling NO_x concentration minus NO concentration.

Over the course of experiments, a gas cylinder containing 5.17 ppm NO in nitrogen gas was used to periodically calibrate the analyzer. After the analyzer output stabilized, the values were recalibrated to 5.17 ppm NO, 0.00 ppm NO_2, and 5.17 ppm NO_x. This was undertaken on a monthly basis while measurements were taken, and at the start of every new measurement campaign.

3. NO_x analysis

3.1 *Measurements at or above 1 mb*

Initial measurements were performed with the low energy table top setup shown in Figure 3, involving discharges in air at tropospheric pressures in order to reproduce previous experiments such as

Wang et al (1998). With the capability to evacuate the chamber to lower pressures, discharges in air at stratospheric pressure were undertaken next. The purpose was to compare the level of NO_x production in discharges at stratospheric pressures (blue jets) to discharges at tropospheric pressures (lightning) and eventually to discharges at mesospheric pressures (red sprites). As shown in figure 9, 500 mb discharges had both a larger amount of NO_x production and a greater rate of NO_x/Ampere (A) of discharge current, as compared to discharges taking place at lowest pressures. This trend continued down to 1 mb, which had the smallest NO_x produced and the lowest NO_x/A.

Discharges at or below 100 mb are linear with current, while 500 mb discharges show more variation. Up to the maximum currents shown, discharge channels for pressures of 100 mb or less were typically straight across the 4 cm discharge gap. At 500 mb, discharges showed some tortuosity, which increased with increasing current.

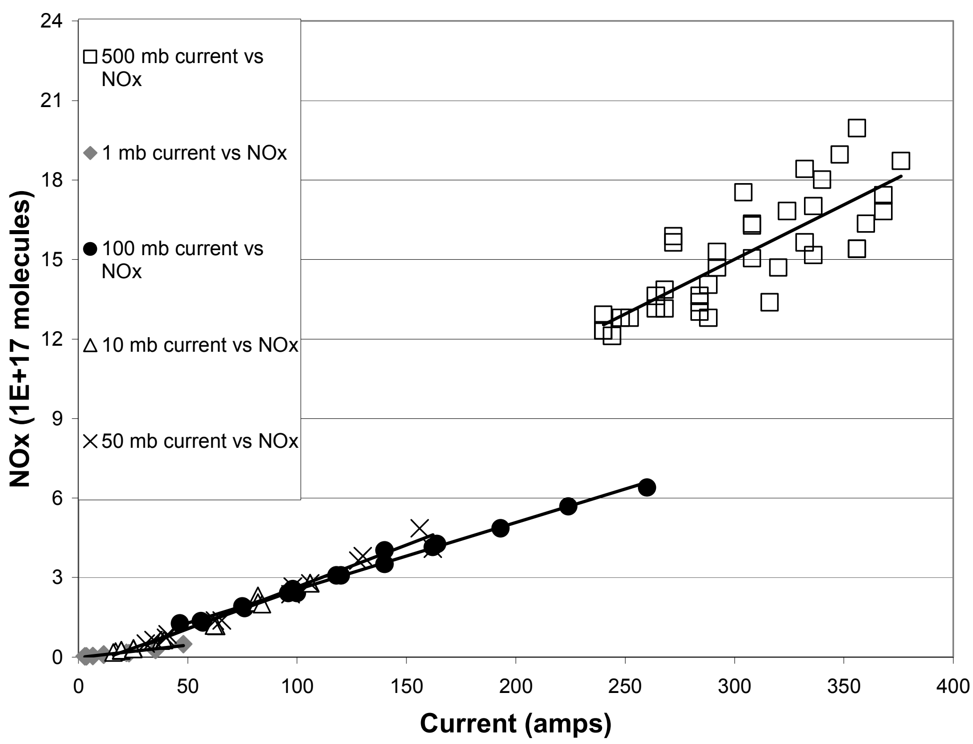

Figure 9: Number of NO_x molecules vs. current for all pressures. Discharges conducted at 500 mb are in one subset, discharges between 10 and 100 mb are in another subset, and 1 mb discharges are in a third subset. Linear fits to each subset of data are included on the graph. These fits were relatively better for discharges at or below 100 mb, as compared to linear fits for 500 mb discharges.

3.2 *Discharge Measurements at or below 1 mb*

In conducting discharge experiments at pressures at or below 1 mb, it was found that NO_x produced by one discharge was too small to be measurable by the NO_x detector. Therefore, measurements of NO_x were only taken after a series of discharges were conducted in the chamber. The number of discharges ranged between 6 and 15 per measurement. NO_x per discharge was calculated as the total NO_x measured divided by the total number of discharges. Linear fits to the components of NO_x produce a reasonable fit for NO_2 production, and a poor fit for NO production, as shown in Figure 10. All regressions also introduced a slight offset error, in that the line/curve did not pass through the origin. For the linear regressions, each discharge is predicted to produce an additional 0.300 ppb NO_x, 0.200 ppb NO_2, and 0.100 ppb NO. These numbers are skewed by the fact that a smaller number of successive discharges will produce a greater fraction of NO_x as NO, while a larger number of successive discharges results in a greater fraction of NO_x as NO_2. Using quadratic regressions, one discharge produces 0.244 ppb NOx, 0.093 ppb NO and 0.07 ppb NO_2, based on the separate quadratic regressions for each component. The quadratic regressions, while introducing the error in adding components, does account for the differing rates of production per discharge for NO and NO_2 as discharge number increases, and closely follows the linear regression for NOx production. Since the linear and quadratic regressions each introduce their own set of errors (as outlined above), both sets of values will be used when calculating production of nitrogen oxides by sprites in the atmosphere.

In comparing NO_x produced by one of these low-pressure discharges to NO_x produced by a sprite, it is important to note the physical differences and similarities. Sprites consist of a series of streamers, each hundreds of meters long. This distance is required for the electrons to reach equilibrium with the surrounding electric field. The discharge gap in the chamber, on the order of centimeters, is much to short for a streamer to form, meaning that chamber air is still in the process of ionizing when these discharges dissipate. However, the electrons are in the process of avalanching, as they would in a

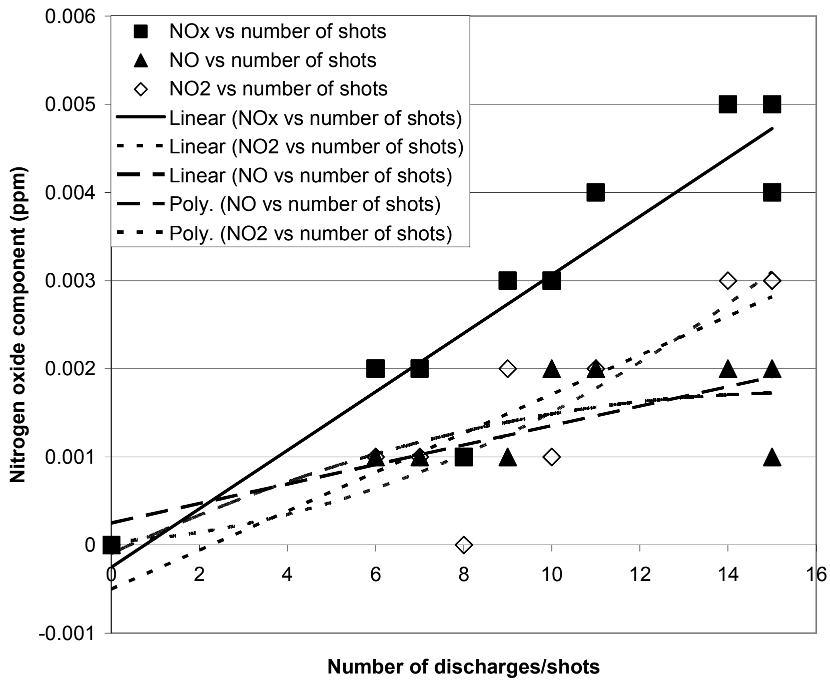

Figure 10: Nitrogen oxides as a function of number of successive discharges. NO_x, NO, and NO_2 production for discharge experiments conducted at 1 mb. NO_x is represented by squares and a solid line, NO is triangles with a long dashed line, and NO_2 is open diamonds with a short dashed line.

streamer. Therefore, the chemical processes in these chamber discharges may be assumed to be the same as those present in a sprite.

In using NO_x production results to determine NO_x production by TLEs, two problems exist. The shape of a blue jet is more easily definable, but the global frequency of blue jets is unknown. Blue jets have been tied to negative cloud-to-ground (CG) flashes, though gigantic jets have been tied to positive CG lightning. Red sprite frequency is known as a fraction of positive CG lightning flashes, but the geometry of a red sprite is irregular. Measurements of multiple streamers through the same space were taken as a partial solution to the latter problem.

3.3 ***Calculation of NOx produced by TLEs in the atmosphere***

Assuming a blue jet to be a cylinder, the volume encompassed by a blue jet may be compared to the volume encompassed by a laboratory discharge, with NO_x/m^3 assumed to be similar (Pasko 2007). The height of a blue jet is taken to be 30 km, based on observations of jets starting at 10 km and terminating at 40 km or higher (Lyons 2000). The diameter of blue jets has not been measured, but can be inferred from the diameter of lightning, as both are leaders (Raizer et al 2006). The lightning channel is initially 1 mm in thickness, with the optically visible portion expanding to 6 cm before it is not bright enough to be seen (Hill et al 1980). This gives a blue jet volume starting at 0.02 m^3 expanding to 80 m^3, taking the lower and upper limits for thickness. By comparison, a chamber discharge with an electrode gap of 4 cm and a thickness of 1 cm has a volume of 3×10^{-6} m^3, for a range of scaling factors from 6.7×10^3 to 2.7×10^6. 100 mb chamber discharges produced 1.3×10^{17} to 6.4×10^{17} molecules of NO_x per discharge. At the lower end of blue jet pressures, 10 mb discharges produced 0.17×10^{17} to 2.8×10^{17} molecules of NO_x per discharge. From this data, a calculated range of NO_x production by a single blue jet event is obtained, with approximately 1.3×10^{20} to 1.7×10^{25} molecules of NO_x produced.

Breaking this down by components, 10 mb discharges produced a minimum of 1.1×10^{16} molecules of NO and 7.6×10^{15} molecules of NO_2 per discharge, while 100 mb discharges 6.0×10^{17} molecules of NO and 4.7×10^{16} molecules of NO_2 per discharge. Therefore, for a single blue jet event, the range of expected NO production is 8.0×10^{19} to 1.6×10^{25} molecules of NO. The range of expected NO_2 production is 5.7×10^{19} to 1.3×10^{24} molecules of NO_2.

Sprite geometry must first incorporate the geometry of individual streamers comprising the sprite, using effective streamer diameters reported by Pasko (2007). Here the effective streamer diameter is defined as the cross-sectional diameter of the streamer if it were compressed into a cylindrical shape. The effective diameter of these sprites can be compared to the dimensions of chamber discharges, leading to similar scales as was previously calculated for sprites.

To find the volume of a sprite so that a scaling factor may be calculated, the shape of a sprite is approximated by two adjoining frustums (Figure 11), or truncated cones. The diameters of the cones are given by the effective streamer diameters at the three heights indicated previously, with the height of the frustums given as the height difference between the set of levels specified. Volume of a frustum is given as:

$$V = \frac{\pi}{12} h D_1^2 (1 - (\frac{D_2}{D_1})^3) \tag{4}$$

, with h as the height, D_1 as the diameter of the base circle, and D_2 as the diameter of the top circle, with a different set of values for each frustum. The bottom frustum will range in volume from 3.47×10^8 m^3 to 1.61×10^9 m^3. The top frustum will range in volume from 8.10×10^7 m^3 to 2.18×10^9 m^3. This makes a combined volume ranging between 4.28×10^8 m^3 to 3.79×10^9 m^3.

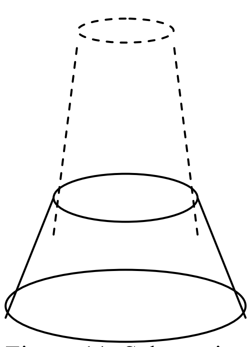

Figure 11: Schematic of two adjoining frustums of differing slant heights. The bottom frustum is given with solid lines, and the top frustum with dashed lines.

For comparison, laboratory discharges in this pressure range also can be approximated by a frustum shape, e.g. upper left of Figure 7, with an upper diameter of 2.0 cm ±0.5 cm and a lower diameter of 3.0 cm ±0.5 cm. The margin of error is such a large percent of the measured value due to the variability of discharges and the inability to directly measure the diameters, with values estimated from camera images. The volume ranged between 5.1×10^{-5} m^3 and 1.1×10^{-4} m^3. As such, the scaling factor ranges between 3.8×10^{12} and 7.4×10^{13}.

As previously mentioned, NO_x production for one of these discharges was 0.1 ppb NO, 0.2 ppb NO_2, and 0.3 ppb NO_x by the linear regression, and 0.093 ppb NO, 0.07 ppb NO_2, and 0.244 ppb NO_x by the quadratic regression. The chamber contains 10.6 L, 0.474 moles, or 2.86×10^{23} molecules of air at room pressure. The production of NO_x was thus 2.86×10^{13} molecules of NO, 5.71×10^{13} molecules of NO_2, and 8.57×10^{13} molecules of NO_x by the linear regression, and 2.66×10^{13} molecules of NO, 2.00×10^{13} molecules of NO_2, and 6.97×10^{13} molecules of NO_x from the quadratic regression. For a single sprite in the atmosphere, NO production will range between 10.0×10^{25} and 2.1×10^{27} molecules. NO_2 production will range between 7.5×10^{25} and 4.2×10^{27} molecules per sprite. Total NO_x production per sprite will range between 2.6×10^{26} and 6.3×10^{27} molecules. Even though a sprite is less energetic than a blue jet, it encompasses a much larger volume, hence the larger NO_x production.

No data is available for determining the global frequency of blue jets in the atmosphere. However, global sprite frequency can be determined from the global occurrence of positive cloud to ground lightning. On average, 15-20% of positive cloud to ground lightning flashes (CGs) are associated with sprite discharges (Reising 1999). Uman (1987) reported that less than 10% of CG lightning globally is positive CG. Similarly, Rakov and Uman (2007) report that no more than 10% of CGs observed globally are positive, citing some studies with an observed frequency as low as 2%. Positive CGs are more frequently encountered during the winter than the summer, with intermediate frequency of occurrence during the spring and fall. The reported frequency has increased in the U.S. over time due to better detection of positive CGs by the National Lightning Detection Network (Orville and Huffines 2001). This indicates that sprite frequency will be between 0.3 and 2% of global lightning frequency.

Orville and Spencer (1979) determined global annual lightning frequency to be 123 flashes per second, as determined from satellite measurements. Christian et al (2003) found a much lower frequency of 44 +- 5 flashes per second, also from satellite measurements. A model study by Price and Rind (1994) found a global flash frequency of 77 flashes per second. Within these bounds, average annual sprite frequency will be between 0.117 and 2.46 discharges per second. Therefore, the average annual rate of NO_x production by sprites ranges between 3×10^{25} and 2×10^{28} molecules per second, with NO production by sprites ranging between 1×10^{25} and 5×10^{27} molecules per second, and NO_2 production ranging between 9×10^{24} and 1×10^{28} molecules per second.

4. Conclusions

An experimental discharge chamber was used to simulate the production of NO_x transient luminous events (TLEs) across a wide range of stratospheric and mesospheric pressures, covering the range of heights at which blue jets and red sprites have been observed to occur. Pasko (2007) shows there are strong similarities between laboratory discharges and TLEs. NO_x measurements from these discharges serve as a first estimate of NO_x production by TLEs.

Analysis of NO_x produced by the discharges was conducted as a function of pressure, voltage, current, and capacitor energy, at pressures corresponding to those in the atmosphere where blue jets and red sprites are encountered. Errors were introduced by coronal discharges producing ozone, and thus a higher proportion of measured NO_2, and so conditions producing corona were avoided. 10 mb chamber discharges were found to produce 0.17×10^{17} to 2.8×10^{17} molecules of NO_x per discharge. 100 mb discharges were 1.3×10^{17} to 6.4×10^{17} molecules of NO_x per discharge. For sprite-like pressures, 7.0×10^{13} to 8.6×10^{13} molecules of NO_x per discharge were produced. These results were analyzed using both linear and quadratic regressions, and were further analyzed by components of NO_x. Using appropriate scaling, blue jets were calculated to produce 1.3×10^{20} to 1.7×10^{25} molecules of NO_x. Red sprites were calculated to produce 2.6×10^{26} and 6.3×10^{27} molecules, which is more than blue jets due to the greater volume encompassed by sprites.

Global NO_x production by sprites was calculated from global lightning statistics. Sprites frequency was determined as a fraction of lightning frequency, specifically 15-20% of positive CGs, and was calculated to be an annual average of 0.117 to 2.46 discharges per second. This results in global annual average production of NO_x by sprites of 3×10^{25} and 2×10^{28} molecules per second. It is concluded that sprite NO_x must be considered in a reliable budget of global nitrogen.

Acknowledgements: This research was sponsored by NSF EPSCoR grant 82725, NSF ATM grant 0224865, NSF SGER grant 6340-663-9070, and by an appointment to the NASA Postdoctoral Program at the Marshall Space Flight Center, administered by Oak Ridge Associated Universities through a contract with NASA.

Bibliography:

Callis, L. B., M. Natarajan, and J. D. Lambeth, 2002: Observed and Calculated Mesospheric NO, 1992-1997. *Geophys. Res. Lett.*, **29**, 2.

Chameides, W. L. et al., 1987: An Estimate of the NO_x Production Rate in Electrified Clouds Based on NO Observations From the GTE/CITE 1 Fall 1983 Field Operation. *Journal of Geophysical Research*, **92**, 2153-2156.

Christian, H. J. et al, 2003: Global Frequency and Distribution of Lightning as Observed from Space by the Optical Transient Detector. *J. Geophys. Res.*, **108**, D1, 4005, doi:10.1029/2002JD002347.

Cohen, R. C. and J. G. Murphy, 2003: Photochemistry of NO_2 in Earth's Stratosphere: Constraints from Observations. *Chemical Reviews*, **103**, 12, 4985-4998.

Cook, D. R. et al., 2000: Production of Nitrogen Oxides by a Large Spark Generator. *Journal of Geophysical Research*, **105**, 7103-7110.

Gerken, E. and U. Inan, 2005: Streamers and Diffuse Glow Observed in Upper Atmospheric Electrical Discharges. *IEEE Trans. Plasma Science*, **33**, 2.

Gordley, L.L. et al., 1996: Validation of Nitrogen Oxide and Nitrogen Dioxide Measurements by the Halogen Occultation Experiment for UARS Platform. *J. Geophys. Res.*, **101**, 10,241-10,266.

Hill, R. D., R. G. Rinker, and H. D. Wilson, 1980: Atmospheric Nitrogen Fixation by Lightning. *J. Atmos. Sc.*, **37**, 179-192.

Huntrieser, H. et al., 1998: Transport and Production of NO_X in Electrified Thunderstorms: Survey of Previous Studies and New Observations at Midlatitudes. *J. Geophys. Res.*, **103**, D21, 28,247–28,264.

Inan, U. S., 2002: Lightning Effects at High Altitudes: Sprites, Elves, and Terrestrial Gamma Ray Flashes. *C. R. Physique 3*, 1411-1421.
Jourdain, L. and D. A. Hauglustaine, 2001: The Global Distribution of Lightning NO_x Simulated On-line in a General Circulation Model. *Phys. And Chem. of the Earth, Part C: Solar, Terrestrial, and Planetary Science*, **26**, 8, 585-591.
Lyons, R. A. et al, 2000: The Hundred Year Hunt for the Sprite. *Eos*, **81**, 373-377.
Oke, T.R., 1999: *Boundary Layer Climates*, second edition, Routledge, Cambridge, Great Britain, 436 pp.
Orville, R. E. and G. R. Huffines, 2001: Cloud-to-Ground Lightning in the United States: NLDN Results in the First Decade, 1989-98. *Monthly Weather Review*, **129**, 5, 1179-1193.
Orville, R. E. and D.W. Spencer, 1979: Global Lightning Flash Frequency. *Monthly Weather Review*, **107**, 7, 934-943.
Orville, Richard E., 1968: A High-Speed Time-Resolved Spectroscopic Study of the Lightning Return Stroke: Part I. A Qualitative Analysis. *Journal of the Atmospheric Sciences*, **25**, 827-838.
Orville, Richard E., 1968: A High-Speed Time-Resolved Spectroscopic Study of the Lightning Return Stroke: Part II. A Quantitative Analysis. *Journal of the Atmospheric Sciences*, **25**, 839-851.
Orville, Richard E., 1968: A High-Speed Time-Resolved Spectroscopic Study of the Lightning Return Stroke: Part III. A Time-Dependent Model. *Journal of the Atmospheric Sciences*, **25**, 852-856.
Pasko, V. P., 2007; Red Sprite Discharges in the Atmosphere at High Altitude: The Molecular Physics and the Similarity with Laboratory Discharges. *Plasma Sources Sci. Technol*. **16,** S13–S29.
Pasko, V. P. and H. C. Stenbaek-Nielsen, 2002: Diffuse and Streamer Regions of Sprites. *Geophys. Res. Lett.*, **29**, 10.
Pasko, V. P. and J. J. George, 2002: Three-dimensional Modeling of Blue Jets and Blue Starters. *J. Geophys. Res.*, **107**, 12.
Peterson, H., M. Bailey, and J. Hallett, Stepped Growth of Ice Crystals in Laboratory Simulated Upper Tropical Troposphere Environments. *Q. J. Roy. Met. Soc.*, in prep., 2008.
Price, C. and D. Rind, 1994: Modeling Global Lightning Distributions in a General Circulation Model. *Monthly Weather Review*, **122**, 8, 1930-1939.
Raizer, Y. P., G. M. Milikh, and M. N. Shneider, 2006: On the Mechanism of Blue Jet Formation and Propagation. *Geophys. Res. Lett.*, **33**, L23801, doi:10.1029/2006GL027697.
Rakov, V.A. and M.A. Uman, 2003: Lightning: Physics and Effects, Cambridge University Press, Cambridge, U.K., 687 pp.
Reising et al, 1999: ELF Sferics as a Proxy for Sprite Occurrence. *Geophys. Res. Lett.*, **26**, 7, 987-990.
Rozanov, E., 2005: Atmospheric Response to NO_y Source Due to Energetic Electron Precipitation. *Geophys. Res. Lett*., **32**, L14811, doi:10.1029/2005GL023041.
Uman, M. A., R. E. Orville, and L. E. Salanave, 1964: The Density, Pressure, and Particle Distribution in a Lightning Stroke near Peak Temperature. *J. Atmos. Sci.*, **21**, 306-310.
Uman, M. A., 1987: The Lightning Discharge, Academic, San Diego, Calif.
Uman, M. A. and R.E. Voshall, 1968: Time Interval Between Lightning Strokes and the Initiation of Dart Leaders. *J. Geophys. Res.*, **73**, 497-506.
Vollhardt, K. P. and N. E. Schore, 1999: *Organic Chemistry: Structure and Function*, third edition, W.H. Freeman and Company, New York, 1210 pp.
Wang, Y. et al, 1998: Nitric Oxide Production by Simulated Lightning: Dependence on Current, Energy, and Pressure. *J. Geophys. Res.*, **103**, D15, 19149-19159.
Wenig, M., et al, 2004: Retrieval and Analysis of Stratospheric NO_2 from the Global Ozone Monitoring Experiment. *J. Geophys. Res.*, **109**, D04315, doi: 10.1029/2003JD003652.
Yair, Y. et al, 2004: New Observations of Sprites from the Space Shuttle. *J. Geophys. Res.*, **109**, D15021, doi:10.1029/2003JD004497.